

Experimental Study of Hydrodynamic Characteristics and Heat Transfer for a Fluid Flow into a Non-Traditional Machining

Raad Muzahem Fenjan

Department of Materials Engineering, Mustansiriya University, Bagdad, Iraq

Email address:

Dr.raad2017@uomustansiriya.edu.iq

To cite this article:

Raad Muzahem Fenjan. Experimental Study of Hydrodynamic Characteristics and Heat Transfer for a Fluid Flow into a Non-Traditional Machining. *Machine Learning Research*. Vol. 3, No. 2, 2018, pp. 18-27. doi: 10.11648/j.ml.20180302.12

Received: August 6, 2018; **Accepted:** August 17, 2018; **Published:** September 13, 2018

Abstract: The non-traditional method used in this work was an electrochemical machining. The experimental work includes designing of machining cell, preparing of fluid solution, selecting the work piece and designing of test rig. The aim of this paper was obtain the gap profile which based on the deviation with respect to equilibrium gap width, also, the electrolyte conductivity deviation with respect to inlet electrolyte conductivity along flow path with the effect electrolyte temperature was obtained for the machining cell. A particular machining cell of two dimensions of (30 mm) width and (50 mm) length, with two dimension turbulent flow for an electrolyte in gap has been selected. For this machining cell, an electrolyte solution (10% w/w NaCl) and the work piece (En8 mild steel) are used. The influence of various parameters, such as supply voltage(12 to 18 volt), tool federate(0.35 to 1.65 mm/min), electrolyte flow rate(5 to 30 lit/min), temperature (40°C) and back pressure (0 to 6 bar) on the gap width and electrolyte conductivity profiles along flow path of the machining cell. The inlet operating parameters for the machining cell were selected within the range of industrially realistic machining circumstances. The optimal control on flow rate and temperature of a electrolyte which refers to gap width without deviation are observed experimentally.

Keywords: Electrochemical Machining, Gap Width, Electrolyte Flow Rate and Temperature, Electrolyte Conductivity, Control

1. Introduction

Optimum ECM process parameters can reduce the its operating and maintenance cost, therefore choice of optimum process parameters is essential to ensure the most cost-effective, efficient, and economic utilization of ECM process potentials. Xiaolong Fang et al., [1], attempted to generate the pulsating flow via a servo-valve in the electrolytic supply pipe, which is introduced to improve the heat transfer, material removal rate and surface profile in ECM. A multi-physics model coupling of electric, heat, transport of diluted species and fluid flow is presented. Simulation results indicate that pulsating flow has a significant impact on the distributions of velocity, gas fraction, and temperature near the work piece surface along the flow direction. M. M. Lohrengel et al., [2], shaped the work pieces are by controlled anodic dissolution at extremely large current densities of about 100 A/cm² in neutral solutions (normally

aqueous NaNO₃). Products were quantified at the electrolyte outlet by on-line photometry or fluorescence quenching and led to detailed models of the interface kinetics. The surface is described as a layered structure of an oxide film and a supersaturated, meta-stable viscous product film which is continuously removed by electrolyte flow. K. P. Rajurkar and D. Zhu, [3], studied the development of a precision ECM process by using an eccentric orbital anode movement with traditional ECM. Theoretical and experimental analyses indicate that orbital ECM distributes the electrolyte flow more uniformly and hence leads to a significant reduction in the flow field disrupting phenomena that adversely affect machining accuracy. Sadineni Rama Rao and G. Padmanabhan, [4], considered three process parameters, namely voltage, feed rate and electrolyte concentration, and one product parameter, percentage of reinforcement, as input parameters. Moreover, the performance characteristics of the process, namely material removal rate (MRR), radial over cut

(ROC) and surface roughness (SR), depends on the process/product parameters and are considered as the responses for this process. Linear statistical models are formulated after conducting the experiments using the concept of full factorial design of experiments. Thanigaivelan, R, [5], This paper investigates the effect and parametric optimization of process parameters for Electrochemical micromachining (EMM) of 304 stainless steel using grey relation analysis. Experiments were conducted using machining voltage, pulse on-time, electrolyte concentration and tool tip shapes as typical process parameters. The grey relational analysis was adopted to obtain grey relational grade for EMM process with multiple characteristics namely machining rate and overcut. Analysis of variance was performed to get the contribution of each parameter on the performance characteristics and it was observed that electrolyte concentration and tool tip shape were the most significant process parameters that affect the EMM robustness. N. K. Jain and V. K. Jain, [6], described optimization of three most important ECM process parameters namely tool feed rate, electrolyte flow velocity, and applied voltage with an objective to minimize geometrical inaccuracy subjected to temperature, choking, and passivity constraints using real-coded genetic algorithms. Comparison of the obtained optimization results with the results of past work in this direction shows an improvement in terms of geometrical accuracy. R. Venkata Rao and V. D. Kalyankar, [7], Thorough literature review of various modern machining processes is presented in this paper. The main focus is kept on the optimization aspects of various parameters of the modern machining processes and hence only such research works are included in this work in which the use of advanced optimization techniques were involved. The review period considered is from the year 2006 to 2012. B. R. Sarkar et al., [8], described the development of a second order, non-linear mathematical model for establishing the relationship among machining parameters, such as applied voltage, electrolyte concentration and inter-electrode gap, with the dominant machining process criteria, namely material removal rate (MRR), radial overcut (ROC) and thickness of heat affected zone (HAZ), during an ECDM operation on silicon nitride. The model is developed based on response surface methodology (RSM) using the relevant experimental data, which are obtained during an ECDM micro-drilling operation on silicon nitride ceramics. From the parametric analyses based on mathematical modelling, it can be recommended that applied voltage has more significant effects on MRR, ROC and HAZ thickness during ECDM micro-drilling operation as compared to other machining parameters such as electrolyte concentration and inter-electrode gap. C Senthilkumar et al., [9], used a multiple regression model to represent relationship between input and output variables and a multi-objective optimization method based on a non-dominated sorting genetic algorithm-II (NSGA-II) was used to optimize ECM process. A non-dominated solution set was obtained. Rajarshi Mukherjee and Shankar Chakraborty, [10], optimized the machining

parameters of an ECM process and a wire electrochemical turning process are using the biogeography-based optimization (BBO) algorithm. Both the single- and multi-response optimization models are considered. The optimization performance of the BBO algorithm is also compared with that of other population-based algorithms. Hansong Li et al., [11], used a 10% NaNO₃ to make multiple holes in Ti-6Al-4V sheets by through-mask electrochemical machining (TMECM). The polarization curve and current efficiency curve of this alloy were measured to understand the electrical properties of Ti-6Al-4V in a 10% NaNO₃ solution. The experimental results suggest that with appropriate process parameters, high-quality holes can be obtained in a 10% NaNO₃ solution. Using the optimized process parameters, an array of micro-holes with an aperture of 2.52 mm to 2.57 mm and maximum roundness of 9 μm were produced using TMECM. Yu Tang and Zhengyang Xu, [12], studied the electrochemical dissolution characteristics of GH4169 under ECM conditions. The open circuit potential, electrochemical impedance spectrum (EIS) and anodic polarization curve are investigated. The polarization curves were measured using an electrochemical workstation and corresponding equations were obtained by computer fitting. Jia Liua et al. [13], Concluded that the excellent performance of gamma titanium aluminium (γ-TiAl) intermetallic makes itself to be a feasible alternative for nickel alloys in aero-engine applications. Orthogonal experiments were conducted to study the effects of process parameters such as applied voltage, electrode feed rate, electrolyte pressure and temperature on material removal rate (MRR), surface roughness (SR) and machining gap (MG) in sodium chloride aqueous solution. The result data of experiments were analyzed by grey relational analysis method. The results indicated that electrode feed rate is the crucial effect on MRR, SR and MG, and the best parameter combination was determined. S. Madhankumar et al., [14], investigated the influence of some predominant electrolytic cavity sinking process parameters such as applied voltage, current, electrolyte concentration, pulse on time, pulse off time and duty cycle on the material removal rate (MRR) to fulfil the effective utilization of ECM of Al 6082, SiC and boron glass powder composites cast by stir casting process. This aluminium matrix composite (AMCs) can be used for making trusses, frames and containers which are used to store chemicals, milk and other corrosive liquids, it can replace stainless steel which is used in the salty environment to avoid corrosion. In this study, the influence on the removal of material, caused by ECM is analyzed. YongCheng Ge et al., [15], employed In this research, electrochemical turning (ECT), which is an extended form of ECM, is to process K423A cast revolving parts. The way of electrolyte-jet is implemented by an inter-jet cathode to improve machining localization and reduce stray corrosion. Simulation results show that the use of electrolyte-jet could effectively suppress the stray corrosion on non-machining areas. The diameter and outlet of the inter-jet cathode, and the cathode feed rate were designed, respectively. Experiments were conducted to

verify the proposed method. It was confirmed that the stray corrosion of the non-machining area can be reduced significantly and the cathode feed rate can also be enhanced by using the proposed method. Finally, a simulated sample of a particular model of cartridge receiver with a larger machining height of 30 mm was fabricated successfully.

2. Experimental Apparatus Layout

The machining system rig is shown in figure 1, also the schematic diagram of the equipment used in the experimental study is shown in figure 2. The tool and work piece, supported by a rigid machine structure and connected to a (D. C.) power supply; where the tool is considered as the cathode and the work piece as an anode. The work piece is fixed and the tool is moved vertically with a controlled linear displacement to give an accurate feed rates. The work piece and tool are sealed in an electrolytic cell through which the electrolyte is pumped under pressure to flow from inlet to outlet at a high velocity by the action of a suitable pump. A (10% w/w) sodium chloride (NaCl) solution used as an electrolyte within a (60 litres) storage tank. After flowing through the machining gap, the electrolyte is returned to the storage tank and carrying the gas bubbles and solid dissolution products. Gas is collected in the storage tank and is extracted to the atmosphere by the centrifugal fan. In The supply tank, the electrolyte is heated to the required temperature by dipping electric heaters and the temperature controlled by a thermostate, also a thermometer is used to record the temperature of the solution. At the outlet of the storage tank, two filters are fitted to prevent particles of dirt or remaining sludge to enter the machining cell. At the entrance pipe to the machining cell, a flow control valve is used to control the pressure and amount of electrolyte entering the cell. Also, flow control valve at the exit pipe from the cell is used to control back pressure during machining. Stable voltage at high machining current is supplied by the electrical power system of the machine. A comprehensive instrumentation system is incorporated to measure voltage, current, feed rate, electrolyte flow rate, temperature and pressure during machining.



Figure 1. Electrochemical machining system rig.

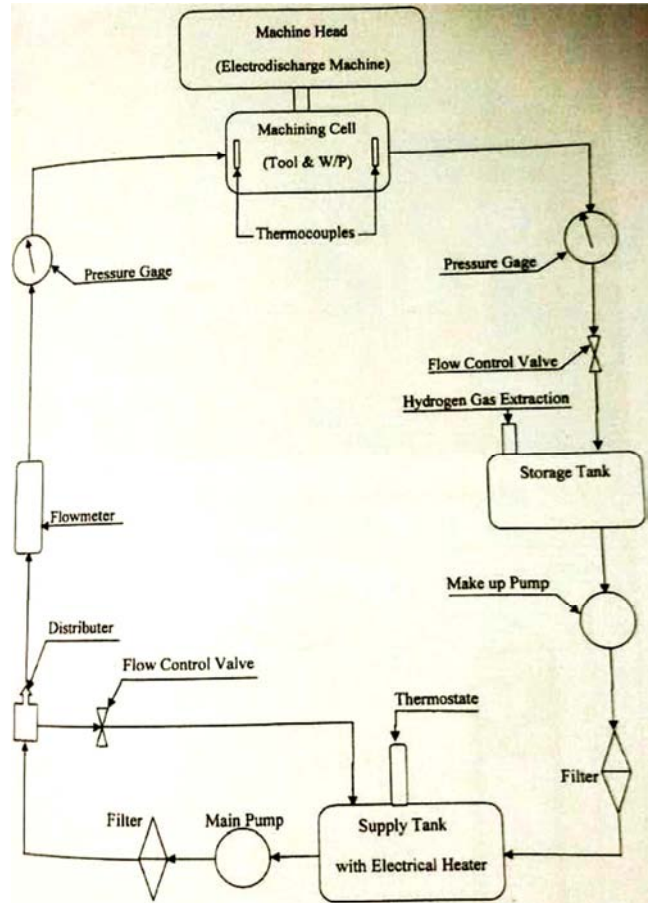


Figure 2. Schematic diagram of the main equipments used in the experimental tests.

2.1. Machining Cell

A machining cell is designed and constructed to confine the electrolyte flow within the working zone whilst allowing the tool to be fed smoothly towards the work piece. Machining cell was chosen with a width of (30mm) and a flow length of (50mm) with curved the edges to reduce the complexity of the hydrodynamic situation by the introduction of edge effects. Figures 3 and 4 show the design and construction of the machining cell to provide the flow channel as mentioned above. The tool was made slightly longer by (1 mm) at each ends to counteract for reduced inter electrode gap at inlet and outlet. All specimens were made from (En8 mild steel) flat steel obtained from the cast, normalised at (950 deg. C), to minimize metallurgical effects. The tool was made in such a way, that it can be fitted and accurately aligned, perpendicularly towards the work piece in the machining fixture with the minimum of setting-up procedure before each test. The work piece base and machining faces were made parallel. Vertical side and end faces of the work piece were also made parallel to each other and square to the machining face using surface-grinding facilities. Work piece fixture, was made so as to clamp the work specimens in accurate alignment with the tool during machining.

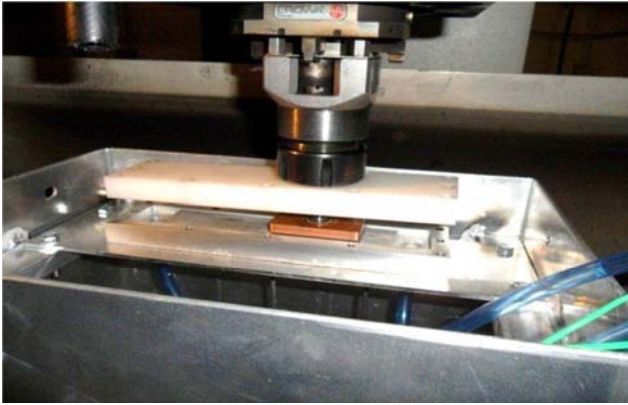


Figure 3. Machining cell picture.

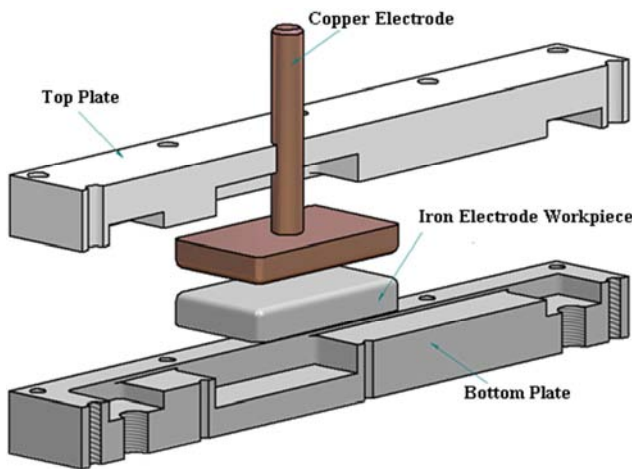


Figure 4. Machining cell schematic.

2.2. Experimental Techniques

The experimental investigation was made to examine the influence of various parameters, such as voltage, tool feed rate, electrolyte flow rate and back pressure on the machining characteristics and profiles developed. Tests were normally conducted at a standard electrolyte conductivity of (0.178 mho/cm) at inlet condition, which was maintained by temperature control at (40°C.).

The conditions for the tests were selected to cover the range of realistic machining circumstances for adequate accuracy of subsequent analysis. Each anode specimen was ground, so that the datum faces were parallel. The work piece was fitted in the fixture and the electrode gap was set as near as possible to the expected equilibrium gap to reduce time delay in reaching the equilibrium condition. The gap was checked at the inlet and outlet points to ensure that the working zone was parallel. The conductivity of the electrolyte was checked, and if necessary, adjusted to the required value stated above. Initial tests were conducted using a tool to establish the relationship for a single phase flow condition through the parallel duct at various gaps, flow

rates and back pressures. Only the pressure at gap inlet and gap outlet was measured by assuming negligible pressure losses at inlet and outlet zones (the work piece inlet and outlet edges were smoothed with a radius similar to that occur during machining).

The effects of various gaps, flow rates and back pressures were examined. In fact the situation of actual machining condition requires modification due to the presence of machining products and the tapering of the equilibrium gap profile. Tests have been conducted, to measure pressure at inlet and outlet of the gap under selected conditions to cover the range of realistic machining circumstances. For each condition, the work piece was machined to equilibrium and the pressure readings were recorded just before the end of the stroke. The electrolyte was then allowed to flow through without tool feed rate. The gap was then measured by taking readings relative to the gap inlet position (because of inlet rounding due to stray machining, this position was taken as (2 mm) from the actual gap inlet). For example, the general steps of a certain test includes pumping the prepared electrolyte from the supply tank to machining cell at the required flow rate, then adjusting the required feed rate of the tool toward work piece, when the required equilibrium gap is achieved, the current machining will be recorded, the work piece was then removed, measured, weighed and the profile deviation was recorded. The work piece profile deviation was measured with the arrangement shown in figure 5. The work piece was moved under the digital dial gauge and readings were taken relative to the inlet position.



Figure 5. Work piece measurement with digital dial gauge.

3. Results and Discussions

Figures 6 and 7 show the gap profile also show the effect of temperature on electrolyte conductivity along the machining length. For each test, two figures are plotted, the first one represents an experimental gap width profiles, while the second figure shows separately the change in conductivity due to temperature and gas effects.

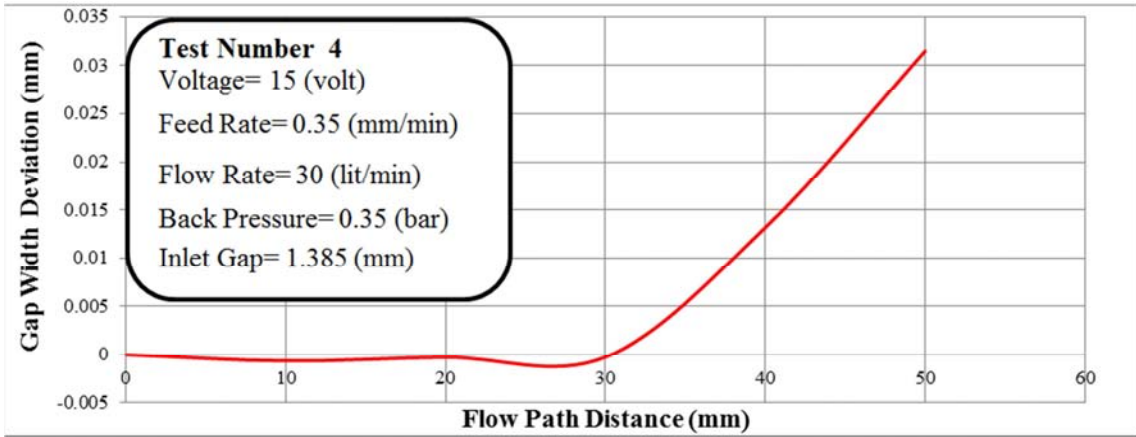


Figure 6. Variation of experimental and theoretical gap width profile along flow path distance from inlet.

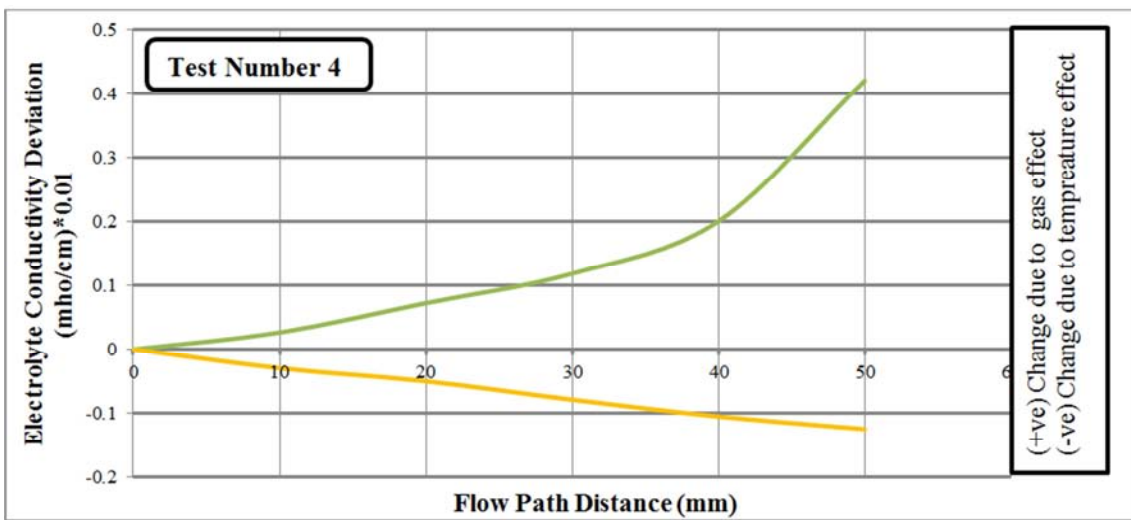


Figure 7. Variation of electrolyte conductivity along flow path distance from inlet.

Figures 8 to 9 show the effect of varying supply voltage, feed rate, flow rate and back pressure during equilibrium machining. For each group, two figures are plotted (first and second), the first one dealt with the variation of the gap along flow path, while the second one dealt with the variation of electrolyte conductivity along flow path.

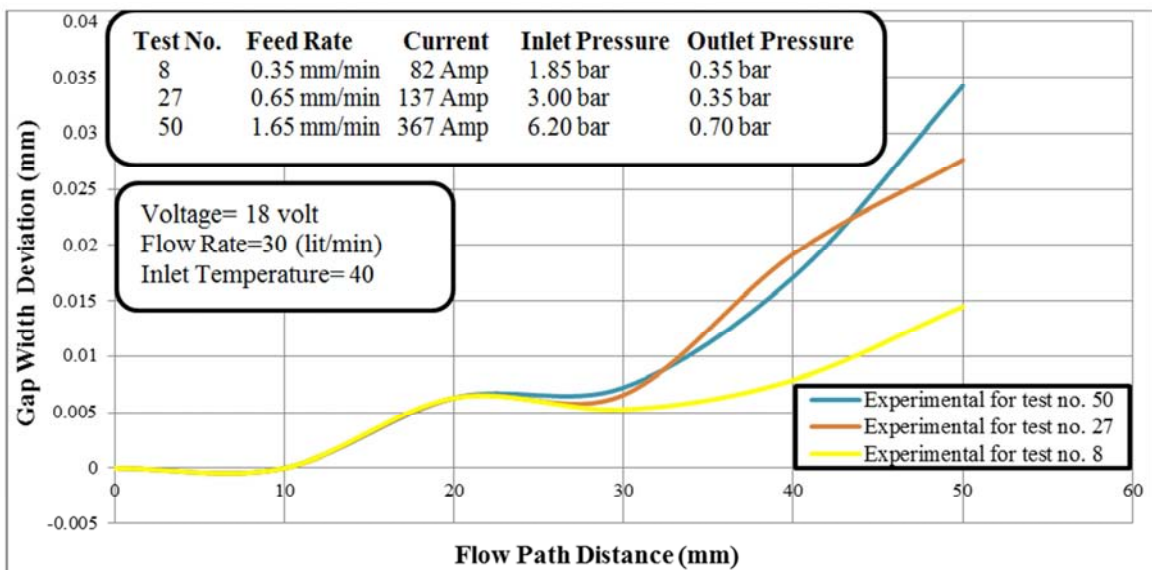


Figure 8. Variation of gap width profile along the flow path for variable feed rates with maintaining the voltage and flow rate constants.

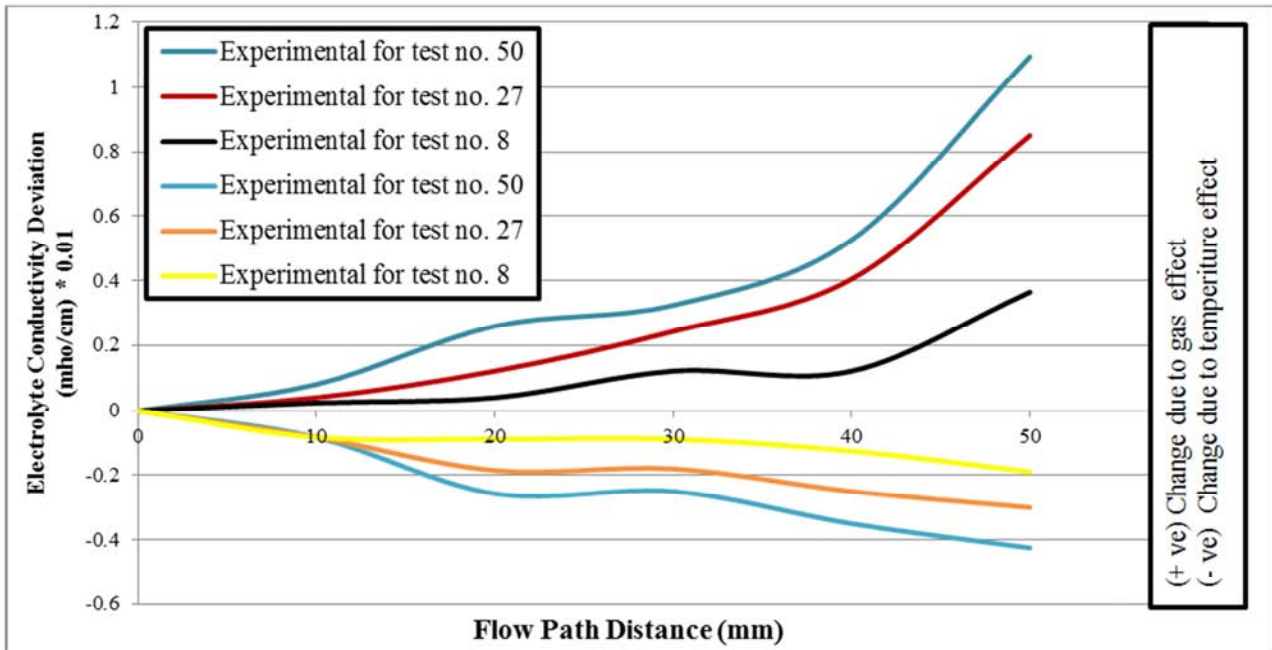


Figure 9. Variation of electrolyte conductivity deviation along the flow path for variable feed rates with maintaining the voltage and flow rate constants.

Figures 10 to 11 show that the gap width variations towards the outlet as supply voltage is varied while maintaining the feed rate and flow rate as constant. These figures show that a decrease in the applied voltage decreases convergence of the gap when compared with other cases using the same flow rate and feed rate without back pressure.

Second figure for each group shows that the outlet temperature rises with voltage with a consequent rise in effective conductivity downstream. The effect of gas on the effective conductivity, for the range of machining conditions considered.

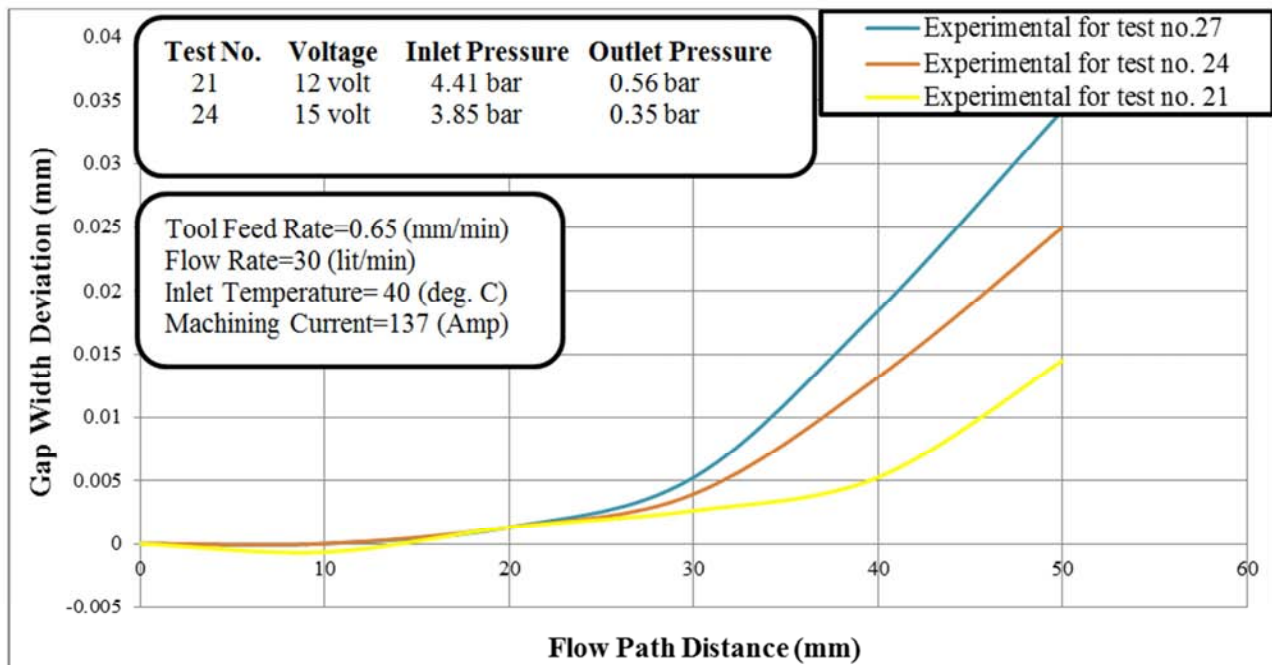


Figure 10. Variation of gap width profile along the flow path for variable voltages with maintaining the feed rate and flow rate constants.

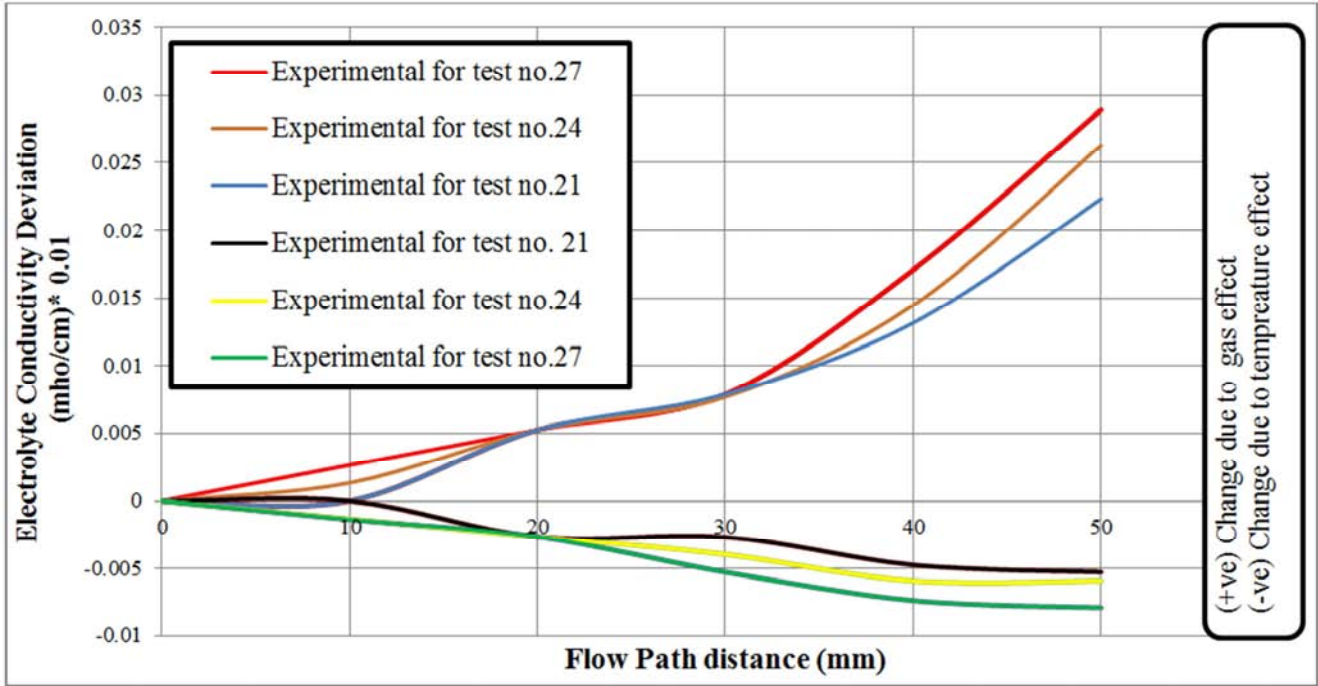


Figure 11. Variation of electrolyte conductivity deviation along the flow path for variable voltages with maintaining the feed rate and flow rate constants.

Figures 12 to 13 show that the gap variations towards the outlet as electrolyte flow rate is varied while maintaining the supply voltage feed rate and as constant. Also, there are two figures (first and second) for each group of the selected tests.

Process conditions for the results presented in these figures were maintained constant. The effective conductivity is significantly reduced.

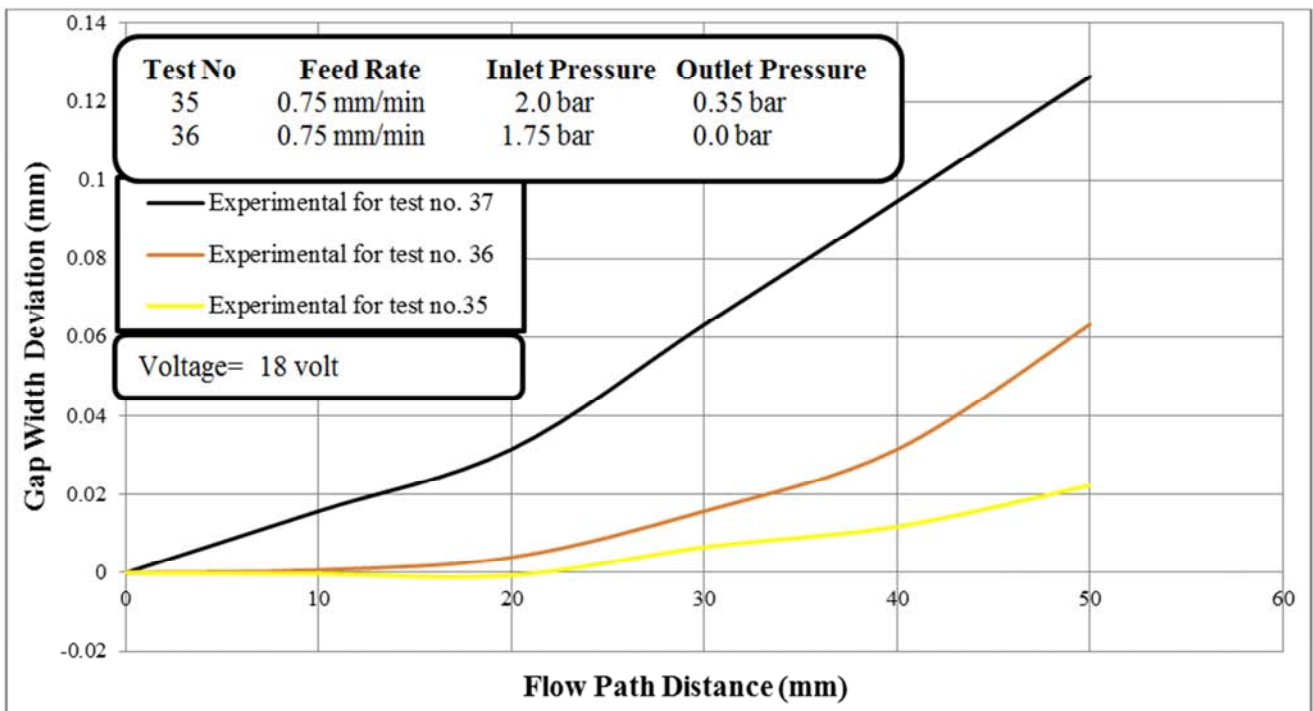


Figure 12. Variation of gap width profile along the flow path for variable flow rates with maintaining the feed rate and voltage constants.

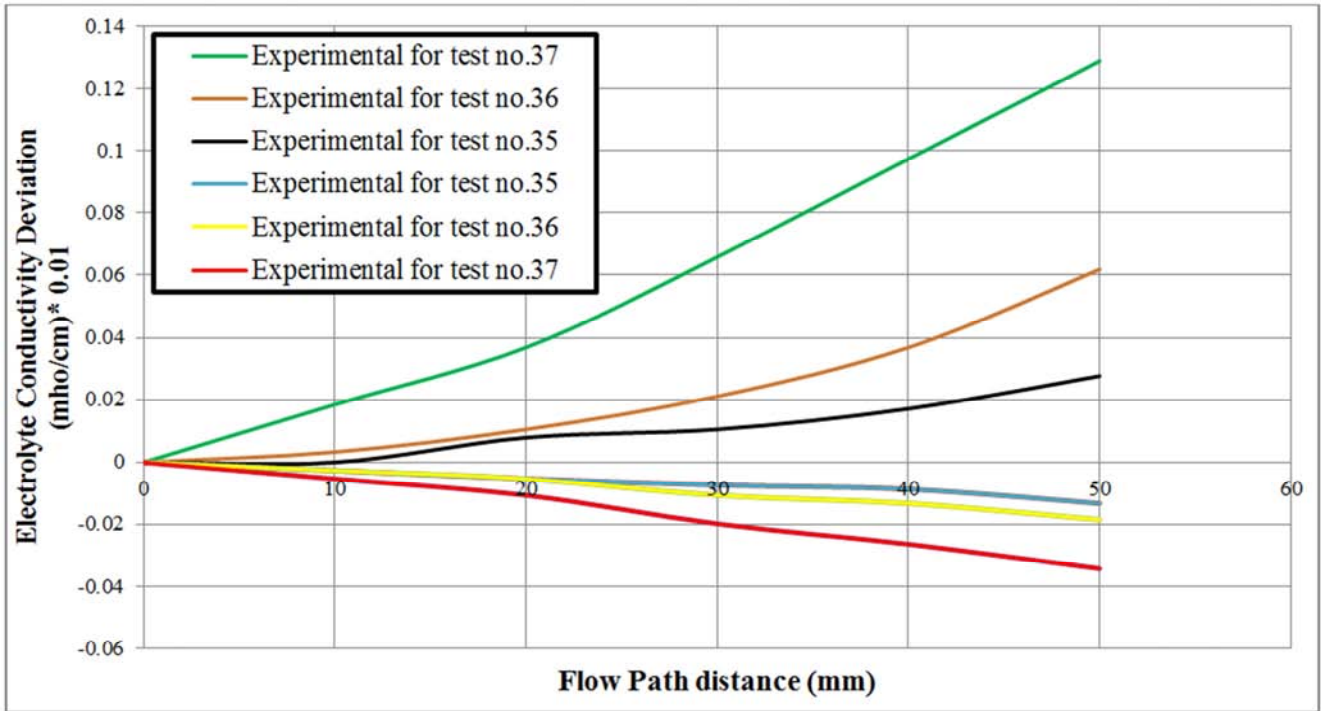


Figure 13. Variation of electrolyte conductivity deviation for various flow rates maintaining the feed rate and voltage constants.

Figures 14 to 15 show that the gap variations towards the outlet as backpressure is varied whilst maintaining the supply voltage feed rate and electrolyte flow rate as constant. Also, there are two figures (first and second) for each group of the

selected tests. As a result, these figures show that the electrode gap decreases towards the outlet as back pressure is increased while the supply voltage, feed rate and flow rate are kept constant.

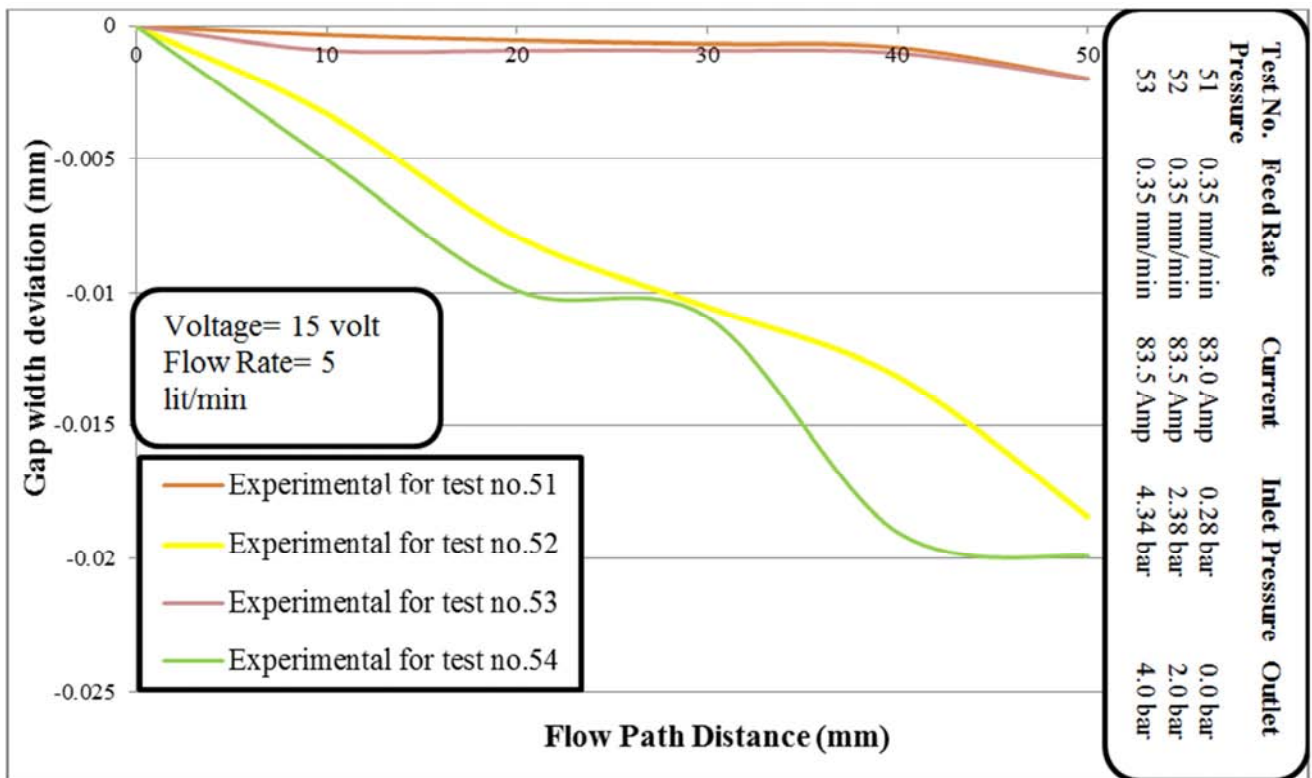


Figure 14. Variation of gap width profile along the flow path for variable back pressures with maintaining the feed rate, flow rate and voltage constants.

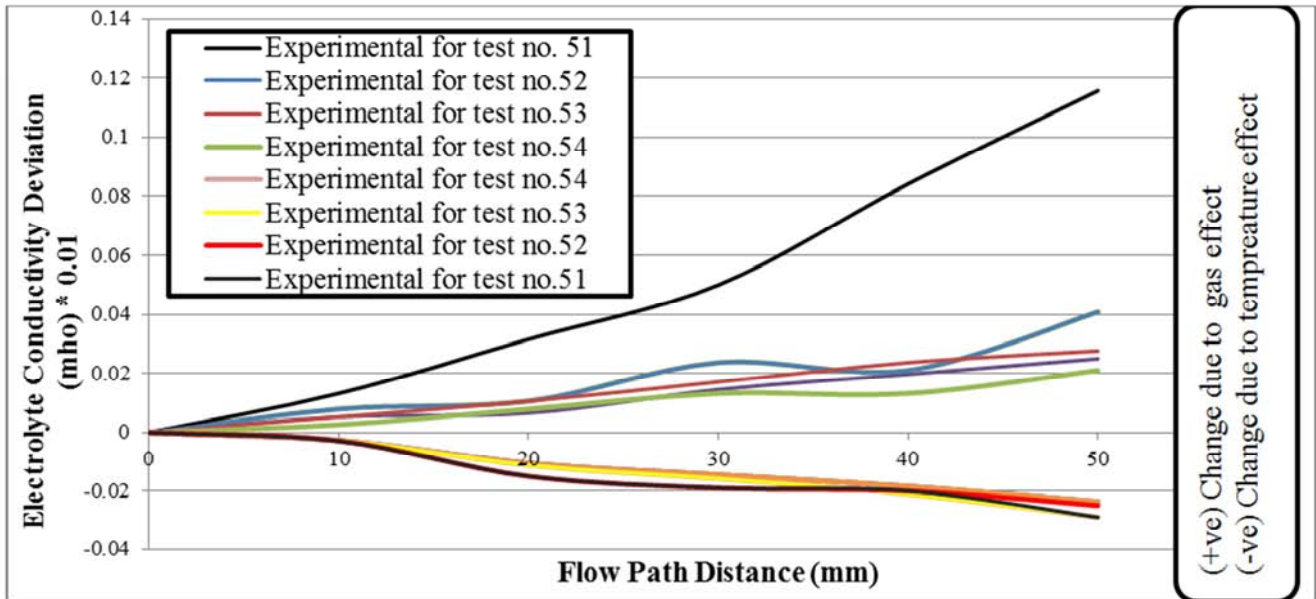


Figure 15. Variation of electrolyte conductivity deviation for various back pressures with maintaining the feed rate, flow rate and voltage constants.

4. Conclusions

Based on the results of investigations under various realistic machining conditions, it can be concluded that;

- 1 The ECM process is described by means of its characteristic relationships, which represent the influence of the process parameters on gap width profile. The process parameters are, machining voltage and current, electrolyte flow rate, pressure and temperature.
- 2 The percentage of ferric reaction in iron dissolution during ECM process can be determined through the study of the energy transfer during electrolytic reaction.
- 3 For pure iron dissolution in sodium chloride electrolyte solution, the sum of electrode potentials and over potentials is, as expected, depends on current density.
- 4 Process efficiency, assuming no evolution of gas at the anode or removal of anodic metal by disintegration, may be expressed as the chemical efficiency.
- 5 Analysis of gap size between inlet and outlet of a flow path has shown close theoretical and experimental agreement when solubility of hydrogen gas is assumed to occur at (100%) current efficiency. Mass of dissolved hydrogen gas will vary with respect to time.
- 6 The application of back pressure during the machining process suppresses hydrogen gas volume effects thereby effectively increasing the downstream conductivity of the electrolyte. An increase pressure increases the volume of gas dissolved into the electrolyte solution.
- 7 The effect of gas evolution on decreasing the conductivity of the electrolyte is more pronounced than the increase in conductivity due to the evolution of heat. It causes a continuous narrowing in the gap width in the direction of electrolyte flow.
- 8 For a given voltage, the current density increases with the increase of the feed rate, this is due to the side

reactions and the variations of the over potential voltage.

- 9 Optimal control on electrolyte flow rate and temperature can be obtained by controlling on the electrolyte conductivity deviation from the electrolyte conductivity at inlet of the machining cell; this controlling leads to control on gap width deviation from the equilibrium gap width.

References

- [1] Xiaolong Fang, Ningsong Qu, Yudong Zhang, Zhengyang Xu and Di Zhu, "Effects of Pulsating Electrolyte Flow in Electrochemical Machining", Journal of Materials Processing Technology, Vol. 214, Iss. 1, pp. 36-43, 2014.
- [2] M. M. Lohrengel, K. P. Rataj and T. Munninghoff, "Electrochemical Machining—Mechanisms of Anodic Dissolution", Electrochimica Acta, Vol. 201, pp. 348-353, 2016.
- [3] K. P. Rajurkar and D. Zhu, "Improvement of Electrochemical Machining Accuracy by Using Orbital Electrode Movement", CIRP Annals - Manufacturing Technology, Vol. 48, Iss. 1, pp. 139-142, 1999.
- [4] Sadineni Rama Rao and G. Padmanabhan, "Linear Modeling of the Electrochemical Machining Process Using Full Factorial Design of Experiments", Journal of Advanced Mechanical Engineering, Vol. 1, pp. 13-23, 2013.
- [5] R. Thanigaivelan and Ramanathan Arunachalam, "Optimization of Process Parameters on Machining Rate and Overcut in Electrochemical Micromachining Using Grey Relational Analysis", Journal of Scientific and Industrial Research, Vol. 72, Iss. 1, 2013.
- [6] N. K. Jain and V. K. Jain, "OPTIMIZATION OF ELECTRO-CHEMICAL MACHINING PROCESS PARAMETERS USING GENETIC ALGORITHMS", Machining Science and Technology An International Journal, Vol. 11, Iss. 2, pp. 235-258, 2007.

- [7] R. Venkata Rao and V. D. Kalyankar, "Optimization of modern machining processes using advanced optimization techniques: a review", *The International Journal of Advanced Manufacturing Technology*, Vol. 73, Iss. 5–8, pp. 1159–1188, 2014.
- [8] B. R. Sarkar, B. Doloi and B. Bhattacharyya, "Parametric analysis on electrochemical discharge machining of silicon nitride ceramics", *The International Journal of Advanced Manufacturing Technology*, Vol. 28, Iss. 9–10, pp 873–881, 2006.
- [9] C. SENTHILKUMAR, G. GANESAN and R. KARTHIKEYAN, "Parametric optimization of electrochemical machining of Al/15% SiC_p composites using NSGA-II", *Transactions of Nonferrous Metals Society of China*, Vol. 21, Iss. 10, pp. 2294-2300, 2011.
- [10] Rajarshi Mukherjee and Shankar Chakraborty, "Selection of The Optimal Electrochemical Machining Process Parameters Using Biogeography-Based Optimization Algorithm", *The International Journal of Advanced Manufacturing Technology*, Vol. 64, Iss. 5–8, pp 781–791, 2013.
- [11] Hansong Li, Chuanping Gao, Guoqian Wang, Ningsong Qu, and Di Zhu, "A Study of Electrochemical Machining of Ti-6Al-4V in NaNO₃ solution", *Scientific Reports* | 6:35013 | DOI: 10.1038/srep35013, 2016.
- [12] Yu Tang and Zhengyang Xu, "The Electrochemical Dissolution Characteristics of GH4169 Nickel Base Super Alloy in the Condition of Electrochemical Machining", *International Journal of Electrochemical Science*, Vol. 13, pp. 1105 – 1119, 2018.
- [13] Jia Liua, Di Zhua, Long Zhaoa and Zhengyang Xu, "Experimental Investigation on Electrochemical Machining of γ -TiAl Intermetallic", *Procedia CIRP*, Vol. 35, pp. 20 – 24, 2015.
- [14] S. Madhankumar, Dr. K. Manonmani, Dr. S. Periyasamy, S. Rajesh and S. Kannaki, "Experimental Study of Effect of Parameters on Material Removal Rate for Electrochemical Machining of Aluminium Matrix Composite", *International Journal of Creative Research Thoughts (IJCRT)*, Vol. 5, Iss. 4, 2017.
- [15] YongCheng Ge, Zengwei Zhu, Zhou Ma and Dengyong Wang, "Tool Design and Experimental Study on Electrochemical Turning of Nickel-Based Cast Superalloy", *Journal of Electrochemical Society*, Vol. 165, Iss. 5: E162-E170, 2018.